Multi-instrumental observations of a positive gigantic jet produced by a winter thunderstorm in Europe

Oscar A. van der Velde,[1] József Bór,[2] Jingbo Li,[3] Steven A. Cummer,[3] Enrico Arnone,[4] Ferruccio Zanotti,[5] Martin Füllekrug,[6] Christos Haldoupis,[7] Samir NaitAmor,[8] and Thomas Farges[9]

Received 3 May 2010; revised 3 August 2010; accepted 11 August 2010; published 16 December 2010.

[1] At 2336:56 UTC on 12 December 2009, a bright gigantic jet (GJ) was recorded by an observer in Italy. Forty-nine additional sprites, elves, halos and two cases of upward lightning were observed that night. The location of the GJ corresponded to a distinct cloud top (−34°C) west of Ajaccio, Corsica. The GJ reached approximately 91 km altitude, with a "trailing jet" reaching 49–59 km, matching with earlier reported GJs. The duration was short at 120–160 ms. This is the first documented GJ which emerged from a maritime winter thunderstorm only 6.5 km tall, showing high cloud tops are not required for initiation of GJs. In the presence of strong vertical wind shear, the meteorological situation was different from typical outbreaks of fall and winter thunderstorms in the Mediterranean. During the trailing jet phase of the GJ, a sprite with halo triggered by a nearby cloud-to-ground lightning flash occurred at a relatively low altitude (<72 km). At the same time, the trailing jet and beads were reilluminated. Electromagnetic waveforms from Hungary, Poland, and the USA revealed this GJ is the first reported to transfer negative charge (approximately 136 C) from the ionosphere to the positively charged origins in the cloud (i.e., a positive cloud-to-ionosphere discharge, +CI), with a large total charge moment change of 11600 C km and a maximum current of 3.3 kA. Early VLF transmitter amplitude perturbations detected concurrently with the GJ confirm the production of large conductivity changes due to electron density enhancements in the D-region of the ionosphere.

Citation: van der Velde, O. A., J. Bór, J. Li, S. A. Cummer, E. Arnone, F. Zanotti, M. Füllekrug, C. Haldoupis, S. NaitAmor, and T. Farges (2010), Multi-instrumental observations of a positive gigantic jet produced by a winter thunderstorm in Europe, *J. Geophys. Res.*, *115*, D24301, doi:10.1029/2010JD014442.

1. Introduction

[2] Gigantic jets (or giant jets) in short GJs are the most recently discovered member in the family of transient luminous events (TLEs). Transient luminous events constitute mesospheric streamer discharges (sprites) and diffuse optical emissions (halos and elves) [*Neubert*, 2003], as well as electrical discharges growing out of thunderclouds toward higher altitudes (jets). In 2001 and 2002, *Pasko et al.* [2002] and *Su et al.* [2003] independently observed the new GJ phenomenon in the form of a large jet shooting from a thundercloud top all the way to the ionosphere with terminal altitudes ~86–91 ± 5 km in the latter case (five events). Subsequent observations [*Hsu et al.*, 2004; *van der Velde et al.*, 2007a, 2007b; *Kuo et al.*, 2009; *Cummer et al.*, 2009; *Chou et al.*, 2007] confirmed previously observed characteristics of the phenomenon: an initial fast development of the full extent of the jet (top altitudes in the range of 70–95 km), a trailing jet, topped by a brighter, long-lasting and slowly rising transition zone (between 45–65 km altitude), and, in some cases, a final rebrightening of the jet. The transition region feature was used for distinguishing a GJ from shorter-lasting sprites at large distances or through less ideal atmospheric conditions [*Hsu et al.*, 2004; *Cummer et al.*, 2009], conditions that may have led to mistake GJs for large carrot sprites or large blue jets in past observations. The upward velocity of the leading jet has been most often reported to be of the order of 10^7 m s^{-1}, but lower velocities, resolved by standard video cameras, have also been reported (~10^5 m s^{-1} by *Pasko et al.* [2002]; 10^6 m s^{-1} by *Su et al.* [2003]). The smaller

[1]Electrical Engineering Department, Technical University of Catalonia, Terrassa, Spain.
[2]Geodetic and Geophysical Research Institute of the Hungarian Academy of Sciences, Sopron, Hungary.
[3]Department of Electrical and Computer Engineering, Duke University, Durham, North Carolina, USA.
[4]Dipartimento di Chimica Fisica e Inorganica, University of Bologna, Bologna, Italy.
[5]Italian Meteor and TLE Network, Italy.
[6]Centre for Space, Atmospheric and Oceanic Science, Department of Electronic and Electrical Engineering, University of Bath, Bath, UK.
[7]Physics Department, University of Crete, Heraklion, Crete, Greece.
[8]Centre de Recherche en Astronomie Astrophysique & Géophysique, Algiers, Algeria.
[9]Commissariat à l'Energie Atomique, Arpajon, France.

0148-0227/10/2010JD014442

sibling of the GJ, the blue jet, reaches significantly lower altitudes (40 km, *Wescott et al.* [1995, 1998, 2001]; 46 km, *Kanamori et al.* [2004]) and exhibits a distinct diverging cone shape, fading with altitude. Its velocity is noticeably slower at ~10^5 m s^{-1} [*Wescott et al.*, 1995]. *Wescott* [1996] noted a bimodal distribution of the terminal altitude of jets, and termed the smaller events (<25.5 km) "blue starters."

[3] Gigantic jets are a long-lasting type of transient luminous event. The duration of GJs mostly depends on the trailing jet stage and whether another "return stroke" occurs (a sudden brightening, or rebrightening, along the entire extent of the discharge). The longest total durations reported were 800 ms [*Pasko et al.*, 2002] and 650 ms [*Su et al.*, 2003]. *Kuo et al.* [2009] presented an analysis of spectral emissions and provided a first conceptual model of the GJ process, explaining the trailing jet feature with a locally lowered ionosphere after the completed GJ stage.

[4] Both gigantic jets and blue jets are rarely observed during ground-based observing campaigns, but in a study of events recorded by the ISUAL instrument in an orbit around Earth covering the latitudes between 45°S and 45°N, sprites occur only a factor of ~60 more frequently than GJs [*Chen et al.*, 2008a]. Given that thunderstorms are most frequent over land, the 0.7:1 land-ocean ratio they found suggests maritime storms are somehow more favorable for GJs. In contrast, global sprite occurrence follows the distribution of thunderstorms. While sprites occur typically over stratiform precipitation regions of mesoscale convective systems [e.g., *Lyons*, 1996; *Williams*, 1998; *Soula et al.*, 2009] as well as clustered winter time convective cells over sea [*Hayakawa et al.*, 2004; *Adachi et al.*, 2005; *Yair et al.*, 2008], the GJ-producing storms reported in aforementioned studies were intense tropical or midlatitude multicell clusters with tops of 14 km or higher. The magnitude of the vertical difference in horizontal wind vectors (vertical wind shear) supported supercells in some cases [*van der Velde et al.*, 2007a]. Supercells are well-organized, long-lived, rotating thunderstorms and have occasionally also been reported to produce sprites [*Lyons et al.*, 2008]. Several observers have taken note that gigantic jets or blue jets occurred over storms in rainbands of hurricanes or typhoons [*Chen et al.*, 2008b; *Tsai et al.*, 2009; *Cummer et al.*, 2009]. Such bands often contain embedded miniature supercells [*Eastin and Link*, 2009].

[5] Gigantic jets can be considered the upward-directed equivalent to a cloud-to-ground (CG) discharge: a cloud-to-ionosphere (CI) discharge. *Petrov and Petrova* [1999] were the first to suggest that a jet could be the continuation of regular lightning leaders into the air above. *Raizer et al.* [2007] showed that development of an upward streamer from the cloud is much facilitated when started by a bidirectional leader tree inside the cloud, which brings the cloud potential to higher altitudes. In their model, however, it was not explained how the discharge could initiate above the upper charge layer. *Krehbiel et al.* [2008] presented a unifying mechanism by which lightning discharges can propagate out of a cloud, including sideward and upward, bearing similarities to the work of *Mazur and Ruhnke* [1998] and *Mansell et al.* [2002] with respect to the development of bidirectional lightning channels in response to distributions of charge in a thunderstorm. The charge relaxation model of *Krehbiel et al.* [2008], and its recent expansion by *Riousset et al.* [2010], were used to study discharge processes induced by major charge centers within the cloud and screening layers at the cloud boundaries. It was shown that when one branch of the bidirectional discharge roots in the region containing the largest quantity of charge, the other branch can pass through an adjacent region of opposite weaker charge and proceed beyond the edges of the cloud, either to ground as a CG or into the sky above as a blue jet or GJ, depending on the location of initiation relative to the charges. In the process, GJs may create a significant atmospheric impact through chemistry in their plasma channels [*Sentman et al.*, 2008] or as source of terrestrial gamma ray emissions [*Pasko*, 2008].

[6] The most common type of thunderstorm has the main positive charge region situated above the main negative charge region, often with a smaller low level positive charge, i.e. a tripolar charge configuration as reviewed by *Williams* [1989]. *Rust and Marshall* [1996] concluded that only about half of measured vertical electric field profiles in the convective part of storms can be interpreted to fit the tripole model. However, *Stolzenburg et al.* [1998] inferred from a large sample of profiles that updraft regions in storms tend to contain four layers of charge, which can be interpreted as the classic tripole plus a negative charge layer on top. *Coleman et al.* [2003] suggested that the complex structure found from balloon measurements through some thunderclouds may be due to a misqualification of charges deposited by previous discharges as charge centers, and reaffirmed that the tripole structure is a good electrical equivalent of the thundercloud.

[7] The discussed tripolar charge configuration would produce negative GJs (−CI) just as it would produce predominantly −CG lightning flashes. Indeed, the polarity of several GJs observed so far has been confirmed to be negative [*Cummer et al.*, 2009; *Su et al.*, 2003; *Krehbiel et al.*, 2008 about Pasko's event] but the transferred quantity of charge varies considerably, from very large 10,800 C km integrated over 900 ms [*Cummer et al.*, 2009], 1,000–2,000 C km [*Su et al.*, 2003] to moderate 630 C km [*Hsu et al.*, 2004], and small <50 C km [*van der Velde et al.*, 2007a]. Note that these values are expressed as charge moment changes, which were inferred from remote electromagnetic field recordings. The net charge involved is found by division by the vertical distance over which it was transferred.

[8] While sprites are observed regularly in the Mediterranean region in all seasons, no GJ had been recorded during several years of *EuroSprite* campaigns (mainly since 2005) or by other observers. Blue jet observations also have been very scarce so far. The reasons are likely both of observational nature (blue events need to be observed from a short distance because their brightness drops rapidly with distance, and the view to the cloud top must be clear) and meteorological nature (charge distributions and upper level storm characteristics). Taking great advantage of the research infrastructure and coordination developed by *EuroSprite* partners [*Neubert et al.*, 2008] the analysis of this unique observation shows that this new case is substantially different from all the previously reported cases of GJs.

2. Observations

2.1. Optical Observations

[9] Optical observations were taken with a portable camera system set up for observations of transient luminous

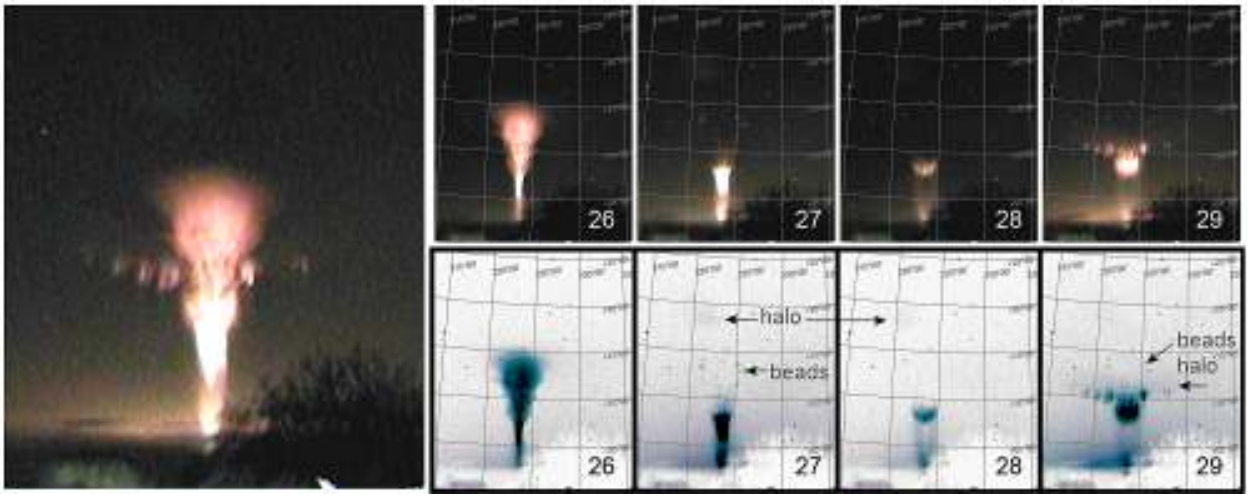

Figure 1. Sequence of video images of the gigantic jet, with frame numbers and azimuth/elevation grid. Each frame lasted 40 ms. The large image on the left is a composite combining the brightest pixels of the video sequence. The bottom row are inverse-brightness images which show better the halo features and beads (annotated) and the diffuse light from the lightning flash. Only a part of the original wide-angle image is displayed. The azimuth-elevation grid spacing is 5°. Images courtesy of co-author Ferruccio Zanotti.

events in Montignoso in the Tuscany region in Italy (44.01°N, 10.15°E). The system is part of the Italian Meteor and TLE Network, which involves amateur observers across Italy and Switzerland (http://www.imtn.it/). The equipment consisted of a Mintron MTV-62V6HP-EX (PAL) 1/2″ color charge-coupled device (CCD) video camera with a 6mm F0.8 wide angle lens (56° field of view). Unlike a typical color camera, the camera did not employ an infrared-blocking filter. The video stream was analyzed by a computer running UFO-Capture event detection software. The software also provided a time stamp and frame numbers for convenience. The PC clock was synchronized every hour to a time server, resulting in an accuracy better than 1 second. The camera was set to 2× accumulation mode (40 ms integration). The camera does this by merging two subsequent odd and even video fields of 20 ms. The interlaced output frames consist of one old image and one new image every 40 ms. This means that either the odd or the even fields can be discarded as all information is contained in each set.

[10] During the night of 12–13 December, a gigantic jet (GJ), displayed in Figure 1, was captured by the camera system at 2336:56 UTC. Between 2226 and 0305 UTC, 37 other transient luminous events, a mix of sprites, elves and halos, were captured in approximately the same direction. 10 transient luminous events were additionally captured over a different storm to the north. A closer convective cloud produced two peculiar upward lightning events from the cloud top. These events reached a top altitude of 7–9.5 km and consisted of multiple simultaneous bright channel stubs, not fading with height, in contrast to blue jets.

[11] The geometrical calculations in this work assume a spherical Earth, adopting the term great circle path (or great circle distance) which refers to the shortest path over the surface of a sphere between two points.

2.2. Lightning and Meteorological Data

[12] Data of two lightning detection networks, the LINET Lightning Location Network [*Betz et al.*, 2004] and the regional networks joined in the European Cooperation for Lightning Detection (hereafter EUCLID), were available to help determine a more precise time interval for the GJ and other transient luminous events. These networks locate lightning by a combination of time-of-arrival and magnetic direction finding techniques in the Very Low Frequency to Low Frequency (VLF to LF, 3–300 kHz) radio range. The detection efficiency is not perfect for either system [*van der Velde et al.*, 2010], between 75% and 90%, and it is lower over the Mediterranean Sea where the event happened. Even strokes with very intense peak currents (e.g., 400 kA) are occasionally missed, and/or wrong polarities are reported as a result of the complexity of intense lightning discharges which do not fit the detection criteria of operational lightning detection services. The differences in peak currents between the systems for the same flashes can range up to 15%, so, the listed values we quote from the systems have to be considered only a rough indication (emphasized also by *Orville* [1999]). 80% of flashes of this night could be geolocated with differences up to 2 km between the locations of corresponding flashes between the two networks for this area of interest (northern Mediterranean Sea), leading to an average location error of about 1 km.

[13] Time series of the east-west and north-south components of the horizontal magnetic field and in some cases the vertical (radial) component of the electric field have been recorded at several receiver stations in Europe and the United States which recorded radio signals in different bands of the Ultra Low to Very Low Frequency range (ULF-VLF, 0.1 Hz–25 kHz). One 1–500 kHz vertical electric field receiver

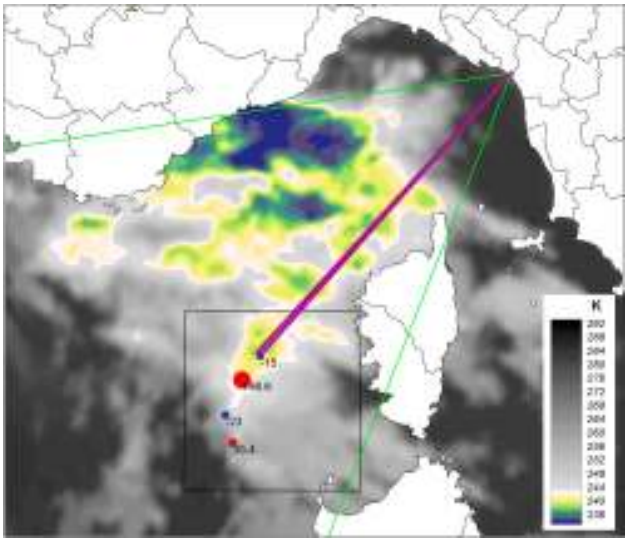

Figure 2. Great circle path from the camera in Montignoso, Italy, to the gigantic jet at a distance of 305 km. The background is the Meteosat cloud top temperature map of 2330 UTC. Cloud tops colder than −30°C have been shaded in color with 1° intervals down to −40°C. Circles are positive (red) and negative (blue) lightning detections by LINET during 2336:56–58 UTC. Their peak current values (kA) are indicated. The field of view of the camera is indicated by green lines. The box is the area of interest used for cloud top and lightning flash rate evolution (Figures 11 and 12).

located in central France was also used. Further details about the stations are included in the Appendix A.

[14] Data from VLF receivers in the Stanford University AWESOME Collaboration (Atmospheric Weather Electromagnetic System for Observation, Modeling, and Education, http://nova.stanford.edu/~vlf/awesome/) have been used to verify ionospheric conductivity disturbances related to the event. These receivers sample the signals of VLF transmitters scattered over the world at 20 ms intervals.

[15] For analysis of the meteorological context of the event, cloud top temperatures were obtained from the 11–13 μm infrared channel of the geostationary Meteosat weather satellite (of EUMETSAT) at 0° longitude, available every 15 minutes. The region of interest is scanned about 2 minutes after the given times. The gridded data provided a resolution of 3.5 km × 4.6 km (16 km^2 per pixel). Radar images from Monte Rasu (Sardinia, 40°25′N, 9°0′E) were obtained and supplied by the Specialistic Hydro-Meteorological and Climatological Department of the Regional Agency for Environmental Protection of Sardinia (IMC-ARPAS). The base scan images covered a range of 250 km, one reflectivity image was available every 30 minutes. Output from the Global Forecast System (GFS) numerical weather prediction model, at 0.5° grid resolution, was available at 3-hour intervals from the United States National Centers for Environmental Prediction. We used the runs of 18 UTC 12 December 2009 and 00 UTC of 13 December 2009 for the general description of the weather pattern and derived convective parameters. A representative radiosonde balloon measurement (sounding) from the station at Ajaccio, Corsica (World Meteorological Organization identifier 07761 LFKJ) was available for 00 UTC on 13 December 2009, containing wind, temperature and dewpoint profile information with altitude.

[16] No additional satellite observations were found in coincidence with this event for studying its chemical impact (e.g., from the ENVISAT satellite, *Arnone et al.* [2009]) or possible gamma-ray emissions [e.g., *Pasko*, 2008].

3. Location and Timing of the Gigantic Jet

[17] A star matching procedure was used to calculate the apparent position of the GJ against the background sky. The lower visible section of the GJ was found to be located at an azimuth of 223°26′ ± 10′ and the diffuse top of the GJ at an elevation angle of about 15°10′. The view was obstructed by clouds below an elevation angle of 2°45′. A first-guess location could be provided by assuming a top altitude of 80–100 km similar to what was found for previous GJ cases [*Pasko et al.*, 2002; *Su et al.*, 2003; *van der Velde et al.*, 2007a, 2007b], placing this GJ west of Corsica at 275–325 km distance from the camera. Note that the Pasko GJ was reported to reach only 70 km altitude, but our reanalysis using the provided data showed this to be based on the distance to the edge of the storm, hence it is a lower bound. The position of their GJ centered on the storm top yielded an altitude estimate of 80–88 km (i.e., 20% taller).

[18] We performed a calibration of the timing of the optical observations. Initial comparison of time stamps in the video frames with sprite-, halo- or elve-triggering +CG flashes, accurately time-stamped by lightning detection networks, indicated that the event time stamp digit was lower by only 0.1 to 0.2 seconds. It was fortunate that the video clip of the GJ also contained a sprite with a halo and some other lightning flashes. The detection listed by LINET of a 198 kA +CG at 2336:56.652 is the trigger of the sprite and halo (41.80°N, 7.46°E) which follows the GJ in video frame 29 which also shows the bright flash. Using this +CG as the main anchor, the beginning and end of video frame 29 (duration 40 ms) surround the +CG time. Two detections at 2336:57.159 and 2336:57.191 of 35 kA and −23 kA correspond to a visual flash later in the video. Since the time interval between detected CGs can fit only in one certain way in the time interval between video frames with flashes, this puts the sprite-producing +CG no further from the beginning of its frame than 13 ms, in other words, frame 29 starts between 56.639 and 56.652 s. This implies that the best estimation of the time of the first frame (26) with the GJ was 2336:56.525.5–565.5 ± 6.5 ms.

[19] LINET presented a first detection at 2336:56.556 (−15 kA) at 41.97°N, 7.63°E, a mere 2.5 km lateral displacement from the great circle path to the GJ. As we will see in the following, it occurred during the leading GJ stage (frame 26), and is therefore likely to have come directly from either the (intracloud or CG) lightning process associated with the GJ, or the GJ itself, so that we could assume its distance (305 km) as the best guess of the GJ location, corresponding to the location 41.99°N, 7.61°E. This location coincides with the coldest cloud top of −34°C. Figure 2 shows the great circle path to the GJ up to 305 km distance and the lightning loca-

Table 1. Dimensions of the Gigantic Jet of 12 December 2009 and the Accompanying Sprite

Vertical dimensions				
Feature	Frame	Elevation ± 10′	Altitude (km) −7% to +3%	Distance used (km)
GJ diffuse top	26	15°10′	91	305
GJ top beads	27, 29	14°00′	84	305
GJ bright stem, lower-upper	26	5°00′–7°40′	34–49	305
GJ transition zone, lower-upper	27	5°35′–8°25′	37–53	305
GJ transition zone, lower-upper	28	7°35′–8°55′	48–56	305
GJ transition zone, lower-upper	29	7°30′–9°35′	48–59	305
Luminous patch (halo, if not cloud)	27–29	18°30′ (azimuth: 221°10′)	111 / 83	305 / 232
GJ lowest visible point (between clouds)	29	1°55′	18	305
Sprite top, center	29	10°50′	72	329 (198 kA CG)
Sprite top, 2341:07 UT	-	12°20′–13°20′	78	307 (406 kA CG)
Elve, 2341:07 UT	-	14°10′	86	307
Horizontal dimensions				
Feature	Frame	Azimuth ± 10′	Width (km) −7% to +3%	Distance used (km)
GJ top section	26	221°27′–225°46′	23	305
GJ transition zone	29	222°05′–224°35′	14	305
GJ trailing jet	28	222°35′–224°35′	11	305
GJ bright stem	26	223°05′–223°45′ (223°26′)	3.7	305
Sprite	29	217°30′–227°50′	60	329

tions superimposed on a background image of satellite cloud top temperatures.

4. Morphology and Development of the GJ and the Sprite

[20] Figure 1 shows the sequence of frames capturing the GJ event. We analyzed the morphological feature altitudes and evolution of the GJ on the basis of the location discussed in the previous section. Table 1 shows the main feature altitudes, calculated with the GJ assumed to be oriented along the vertical at its own location. The distance error margin ranges from 285–314 km and the error in dimensions of morphological features ranges from −7% to +3% on the quoted values, because the precise position is unknown, but most likely associated with the colder convective cloud tops, as was assumed by all GJ work to date. The diffuse top of the GJ reached 91 km, beads 85 km, and the bright top of the trailing jet (also called transition region) slowly moved upward between 37 and 59 km at about 6×10^4 m s^{-1}, remaining luminous for up to 160 ms around 49 km altitude.

[21] The event started with a weak flash in the cloud (frame 25) followed by the completed GJ one frame later (26). No initial streamers can be confirmed that stand out above the image noise level in frame 25. The GJ consisted of a narrow stem (3.5–4 km wide) and a wider upper part (23 km) with streamer structure becoming more diffuse with height. The central part of the stem is bright and there are loops between lower and middle sections. During the completed GJ frame, the light of the causative lightning flash was much brighter. The lowest part of the jet (<22 km) is obscured by clouds. The next frame (27) shows a broadening lower half of the jet while the fanning top section disappeared, except for a few beads. During this frame the brightness and dimensions of the flash increased to a maximum. The following frame (28) is characterized by a widening trailing jet (now 11 km wide) of weaker luminosity, with a hollow look, feeding into a brighter central transition zone feature (14 km width). The beads in the upper section disappeared. The lightning flash intensity was much reduced. The next frame (29), a sprite accompanied by a halo was triggered by a +CG flash 24 km away, which itself is also clearly visible by its light intensity. The columniform sprite has an unusual aspect ratio, with a vertically shallow development compared to the horizontal size of the group, and appears to lack elements near the location of the trailing jet. Remarkably, the transition jet part was re-illuminated, as well as the beads. The lower section of the jet remained at the same brightness and hollow appearance. The sprite top altitude corresponding to a location above the +CG would be 72 km, which is about 5 km lower than the typical initiation height of sprites [*Stenbaek-Nielsen et al.*, 2010; *Stenbaek-Nielsen and McHarg*, 2008] and other sprites that night. If the sprite occurred at the location of the GJ instead, its corresponding top altitude was 66 km. If instead the GJ occurred at the location of the sprite-triggering +CG at 329 km distance, features would turn out 9% larger/higher.

[22] Another transient feature, not previously documented, is a luminous patch at 18°30′ elevation, with the size and luminosity of a sprite halo, slightly horizontally displaced from the GJ. It makes its entry in frame 27 during the bright "half" GJ. Its luminosity reduces over the next two frames. It is faintly visible also during the sprite. Its luminosity behaves independently of the brightness of the lightning flashes, and therefore it seems unlikely that it is a reflection of light on a small cloud. Its height would correspond to 111 km if its distance were the same as that of the GJ. This feature would have an altitude of about 83 km, like a sprite halo, if its distance would be 232 km from the camera where its great circle path crosses a different high cloud top. However, not a

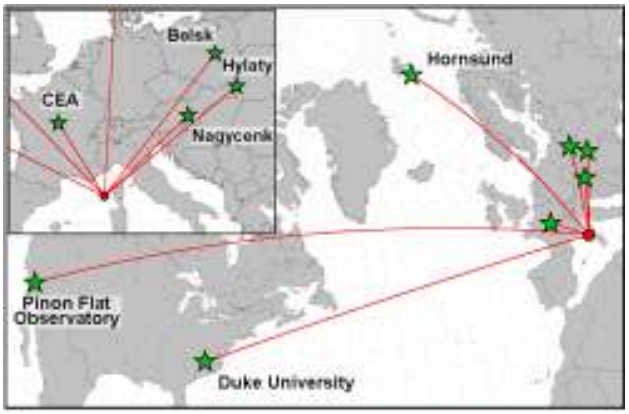

Figure 3. Map showing the locations of the electromagnetic receiver stations used for studying the charge transfer processes associated with the gigantic jet and the sprite which are located at the large red solid dot.

single lightning detection occurred in this area after 21 UTC. If this is indeed a halo during the GJ it suggests the charge removal occurred over a very large area including this closer cloud.

[23] This GJ was registered by an uncalibrated color camera without an infrared blocking filter. Given the problems of unknown white balance and significant near-infrared contamination, it is difficult to make firm conclusions about the absolute colors of the event. The images have first been converted back to the linear response of the sensors. In the unsaturated sections, the red color channel contained the highest values across the entire jet, including the lowest section. The reddest parts in the top section of the GJ and the sprite have a ratio of about 3:1 to 4:1 red to blue in linear color space. The lowest section of the jet contained a slightly lower red content than the top section, with about 2.2:1 red to blue, but this is also the case for the scattered light of the lightning flash above the cloud. The lack of blue was certainly expected because of the long propagation path of the light through air and the low response of a typical color CCD to deep blue and violet light.

5. Electromagnetic Signals

5.1. Ultra-Low to High-Frequency Radio Signals Associated to the GJ and Sprite

[24] Electromagnetic signals in the ULF\ELF\VLF\LF\MF\HF bands were recorded at multiple stations in Europe and overseas. Figure 3 shows a map of the receivers relative to the event location. Figure 4 shows the signals obtained from the

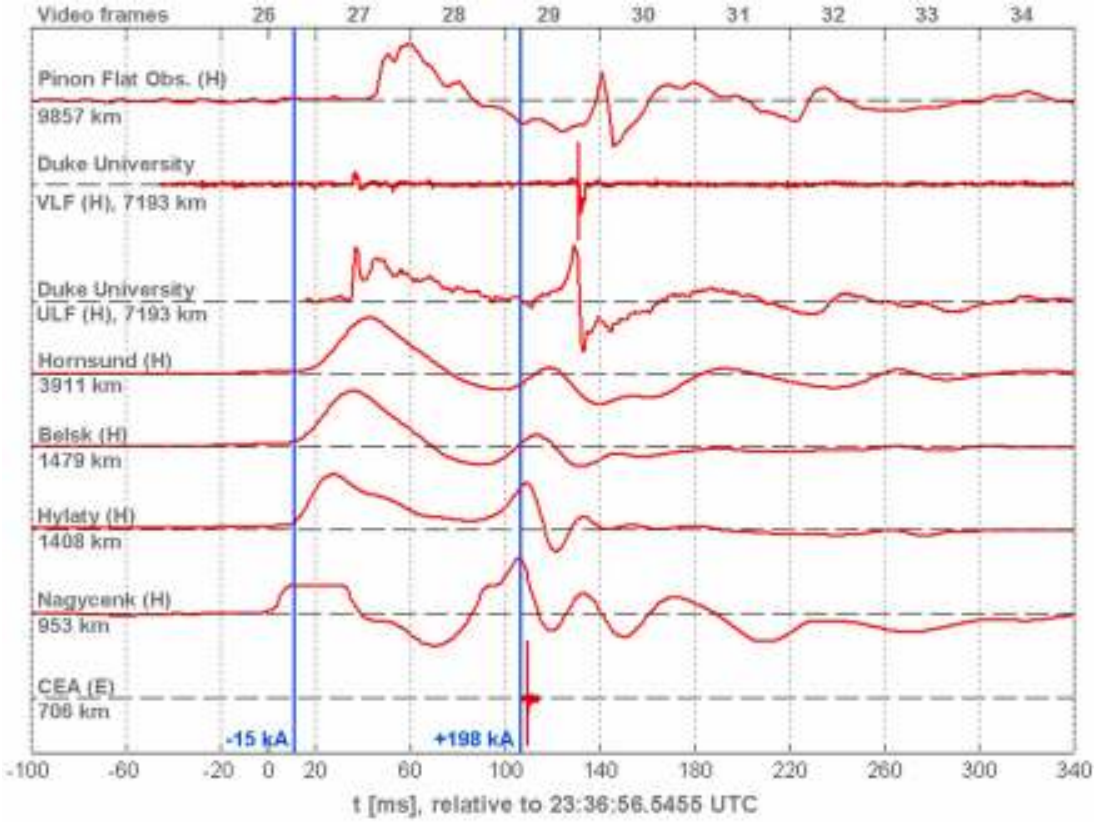

Figure 4. Waveforms of the magnetic field (H) or electric field (E) in the ultra low to high frequency bands as received by the stations displayed in Figure 3, sorted by event-to-receiver distance, with LINET time markers. The top scale indicates the video frames of 40 ms duration, corresponding to those in Figure 1. The signal following the −15 kA lightning detection is attributed to the gigantic jet.

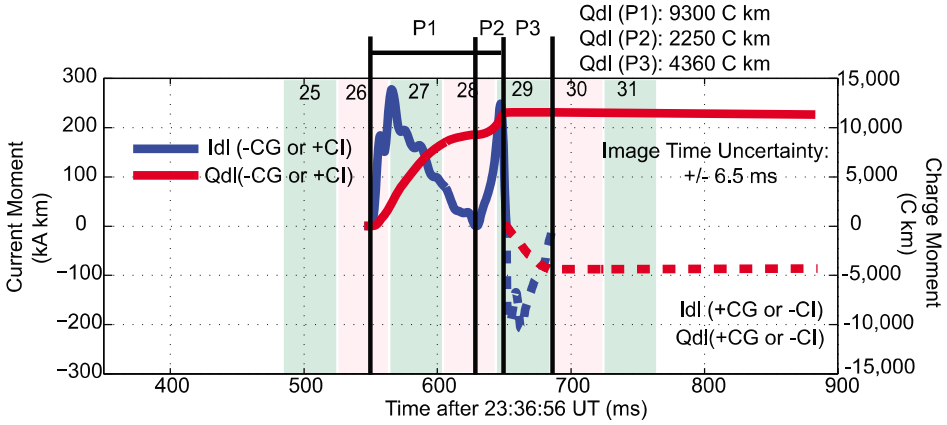

Figure 5. The current moment (Idl) extracted from the waveform of Duke University. Integrated charge moment changes (Qdl) for each polarity signal are indicated by dashed lines. P1, P2 and P3 are periods of interest discussed in the text. The time scale indicates the video frames of 40 ms duration, corresponding to those in Figure 1.

receivers, with the zero time reference at 2336:56.545.5 seconds, the central time of video frame 26 with the first appearance of the GJ. The LINET-detected events of −15 and +198 kA are also marked. The figure shows the large consistency between signals obtained at different locations. It is evident that the detection time of the events is more and more delayed with the growing source-observer distance. The detection at Duke University is earlier because of high frequency signals detected by the receiving system of wider bandwidth. The group velocity of very low frequency waves is 0.991 c (c is the speed of light in vacuum) in the Earth-ionosphere waveguide [*Dowden et al.*, 2002] while the propagation speed of extremely low frequency waves is lower, about 0.8 c [*Chapman et al.*, 1966]. Propagation effects can also be noticed if recorded waveforms from Nagycenk, Belsk, and Hornsund are compared (having approximately the same passband), for example the broadening of the peaks due to dispersion can be observed as the distance from the source grows.

[25] The timing of signals with respect to the GJ and sprite video frames indicates that the first peak, which radiated mostly in the ultra to extremely low frequency bands, is related to the GJ and/or to the lightning discharge which has initiated it. The positive polarity of the signal implies downward motion of negative charge, as in a −CG, or a positive cloud-to-ionosphere discharge (+CI). The second signal is bipolar and is represented strongly also in very low frequency. It can be attributed with certainty to the +CG discharge which produced the accompanying sprite. In the very low to medium frequency range of the CEA station (the closest to the source region), only the second signal surpassed the minimum triggering threshold of 2 V m^{-1}. When zoomed in to the millisecond scale, this signal resembles closely those of other +CG that night. The first detected stroke of −15 kA precedes the main charge transfer that can be attributed to the GJ by less than 1 ms in Duke receiver data. Also in other receiver data, the time interval between the rise of the first and second peaks shows that the detected −15 kA stroke must have occurred during the onset of the first broad peak. It may be tempting to associate the large continuing current to this stroke, meaning a transport of a large amount of negative charge from the cloud to the ground. Large negative lightning continuing current commonly occurs in oceanic thunderstorms across the globe and excites Earth-ionosphere cavity resonances [*Füllekrug et al.*, 2002]. The GJ, however, occurs simultaneously with the observed electromagnetic signal. The GJ observed by *Cummer et al.* [2009] features a similar charge transfer, yet with opposite polarity, during the GJ, such that there is substantial support that the signal indeed originates from the current flow within the GJ and not to ground in the detected stroke. Because it is not uncommon for an operational lightning detection system to misqualify strong intracloud flashes as weak +CGs in normal-polarity storms [*Cummins et al.*, 1998], our conclusion is that the detected weak negative stroke comes from the GJ's parent intracloud lightning (given that the storm is of inverted polarity, section 6), while the large current flows in the GJ itself.

[26] From the raw data of the Duke and Pinon Flat receivers a current moment waveform was extracted, using Finite Difference Time Domain and Schumann resonance models. The Schumann resonance model shows that the ripples in the ULF data after 56.720 sec are the multiple around-the-world pulses. The current moment and cumulative charge moment change waveforms at the location of the event in relation to the video frames are presented in Figure 5. The figure shows that the positive current (upward) at the beginning, during period P1 in the graph, is presumably the current flowing in the body of the GJ. It lasts 72 ms with a peak amplitude of about 280 kA km (implying a 3.3 kA current integrated over the length of the GJ channel) and the total charge moment change is about 9300 C km. During period P2, the positive current increases again for 23 ms (2250 C km). As the +CG occurs, the signal polarity changes from positive to negative, lasting ~30 ms (period P3). It produced a charge moment change of 4360 C km, big enough to cause short-delayed sprites [*Hu et al.*, 2007; *Li et al.*, 2008]. Frame 29 clearly shows the sprite. Since the magnetic field caused by two

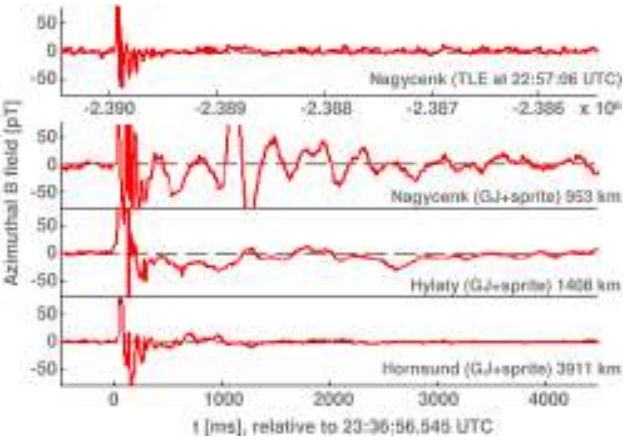

Figure 6. Ultra low frequency waveforms at the time scale of 5 seconds, showing the long resonances after the gigantic jet event (at approximately $t = 0$) at receivers at increasing distance to the event. The top row shows a waveform of a typical sprite for comparison.

oppositely directed currents can cancel each other, the positive current may still exist during the time of the negative current (+CG). It is noted that similar current moment calculations for the measurements at Duke and Pinon Flat differ by a factor of ~2, which could be related to the assumed ionospheric conductivity profiles. A novel method of reconstructing the current moment waveform of the GJ of the Hylaty receiver is to be presented in a forthcoming paper (A. Kułak and J. Młynarczyk, A new technique for reconstruction of the current moment waveform related to a gigantic jet from the magnetic field component recorded by an ELF station, submitted to *Radio Science*, 2010).

[27] At Nagycenk, Hungary, at 953 km from the event, and less pronounced also at receivers farther away, the magnetic field remained disturbed for 3.5 seconds after the event (Figure 6). Waveforms for other transient luminous events (sprites and elves) that night were inspected and none showed this phenomenon. The observed phenomenon has similar characteristics as the ultra slow tails in the ultra low frequency band observed by *Füllekrug et al.* [1998] following some extremely intense sprite-producing lightning discharges. It was shown that those ultra slow tails were likely signatures of ionospheric Alfvén resonances initiated by the parent discharge and/or the accompanying sprite. According to *Shalimov and Bösinger* [2008], "the sufficient excitation of ionospheric Alfvén resonances is thought to be due to (distant) +CG having large peak and long-lasting, strong-continuing currents associated with the discharge," which was certainly the case here. The 2.5–3.5 s duration of the magnetic disturbances observed after the GJ agrees well with the average length of ultra slow tails. Also the dynamic spectra and very weak ellipticity of the signals are supportive of ionospheric Alfvén resonances. The absence of

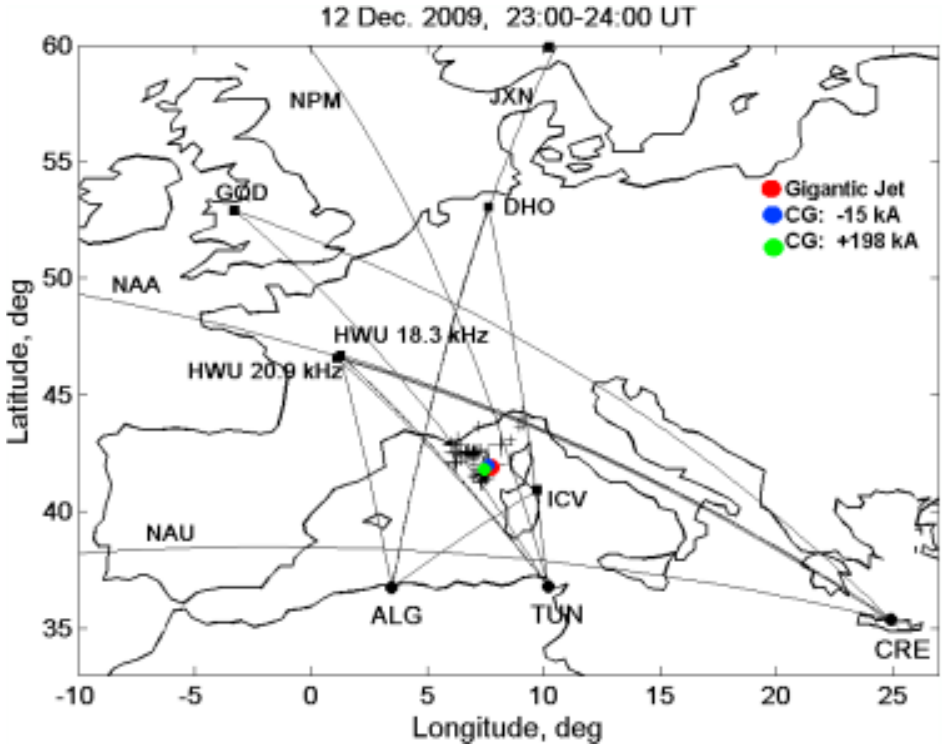

Figure 7. Map showing the locations of the observed +CG lightning discharges during part of the storm that produced the gigantic jet. Also shown are the location of three very low frequency receivers, in Algiers, Tunis and Crete, and various transmitter-receiver great circle paths passing near and around the storm. The narrowband signals of these transmitter-receiver pairs were inspected for the identification of any Early type VLF perturbations that occurred in relation with the gigantic jet.

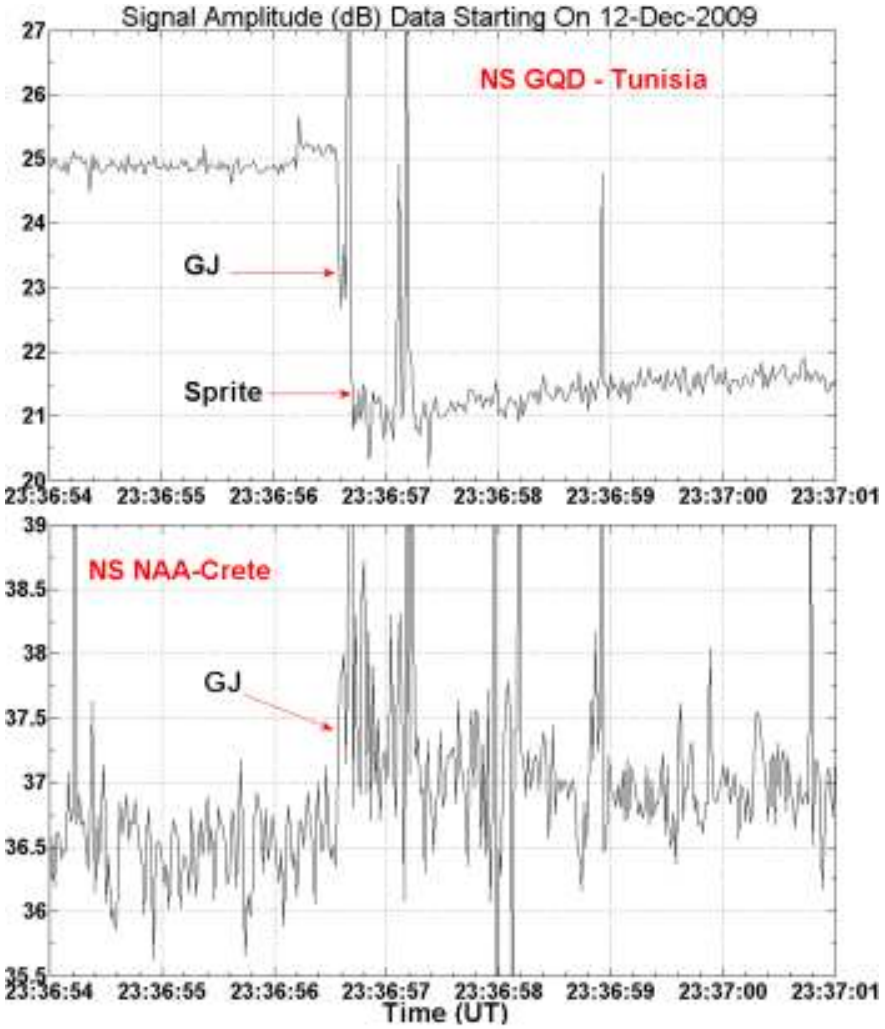

Figure 8. Narrowband amplitude signal recordings from the GQD-Tunis and NAA-Crete VLF transmitter-receiver paths links (north-south field components). The *y*-axes show the relative VLF signal amplitude in dB. These were the only two links that detected rather strong Early-fast type VLF perturbations which initiated approximately at the gigantic jet onset.

such signatures in the recorded time series of the E_z field is due to the narrower bandwidths and higher noise level of the electric data channels of the recording systems. The magnetic disturbances cannot be unambiguously assigned either to the first extremely low frequency pulse or to the bipolar signal because of their close overlap.

5.2. Early VLF Perturbations in Relation with the GJ and Sprite

[28] To investigate if the GJ is accompanied by conductivity perturbations in the D-region of the ionosphere, the very low frequency (VLF) recordings of the Stanford-AWESOME network receivers, which monitor the amplitudes of radio waves from VLF transmitters with great circle paths passing near the GJ location, were inspected. Figure 7 provides geographic information on the location of the storm that produced the GJ, as well as the VLF receiver locations and the transmitter great circle paths to the receivers that have been analyzed for the identification of Early VLF perturbations. Early type VLF events are abrupt perturbations in the signal amplitude and/or phase of a subionospheric VLF transmission that is received at a location. The term "early" signifies the nature of these perturbations, meaning that they occur right after a cloud-to-ground lightning discharge through the effects of its electrical impact onto the lower ionosphere. For more on Early VLF events see the recent review by *Inan et al.* [2010]. The storm area in Figure 7 is confined here by the locations of the +CG discharges (crosses) seen during the 23 to 24 hours UTC interval, and the positions of the 15 kA −CG (blue dot), the 198 +CG (green dot) discharges both situated near the GJ location (red dot). As discussed previously, the −CG discharge that appeared at 2336:56.5560973 UTC occurred at about the same time as the GJ onset. The large +CG discharge of 198.6 kA (located at 41.80°N, 7.46°E) came ~105 ms later at 2336:56.6517839 UTC and is causative of the sprite that appeared superposed in frame 29. The nearest VLF path to the storm, which is therefore expected to be affected the

most if a perturbation in D-region electron conductivity happens, is the GQD-Tunis pair whose great circle path crosses through the storm region, passing less then ~50 km to the southwest of the estimated GJ position. As shown below, this is the path that has seen the strongest VLF perturbation which occurred in association with the luminous activity starting at the GJ onset.

[29] The inspection of the VLF signals for the paths seen in Figure 7, all made with a sampling interval of 20 ms, led to the detection of an Early type VLF perturbation that started at the same time as the GJ and was further strengthened by the subsequent sprite. This composite event was detected only in two paths, that is, the GQD-Tunis and the NAA-Crete ones, whereas a much weaker perturbation was also recognized to occur in the DHO-Algiers path (not shown). Figure 8 displays narrowband receiver recordings for the GQD-Tunis and the NAA-Crete paths during a 7 s time interval from 2336:54 to 2337:01 UTC, centered at about the GJ occurrence time. The Tunis signal shows an abrupt negative perturbation of about 2.0 dB to initiate at about the time of the −CG sferic and the GJ onset. This has been followed by a second jump up to the uncommonly large level of 4 dB that occurred coincidently with the second sferic that relates to the sprite causative +CG of 198 kA. This sequence is also present, but less clearly, in the weaker positive perturbation of ~0.8 to 1.2 dB seen in the NAA-Crete path signal. These sequential occurrences may not be easily resolvable in the time series shown in Figure 8 but they have been inferred to have occurred with certainty in time series plots of shorter duration. A detailed analysis of the VLF data is to be presented in a forthcoming paper.

[30] These data document for the first time that a GJ is accompanied by an Early VLF perturbation caused by conductivity modifications in the overlying D-region of the ionosphere. This observation implies that a production of ionization, and thus an enhancement of electron density, has occurred in conjunction with the GJ, as it also happens nearly always with sprites (e.g., *Haldoupis et al.* [2010]).

6. Meteorological Context and Characteristics of the Storm, Lightning Activity

[31] Previous cases of GJs have been associated to tall tropical or subtropical thunderstorms with cloud tops reaching high altitudes of 14–18 km [*Pasko et al.*, 2002; *Su et al.*, 2003; *van der Velde et al.*, 2007a, 2007b; *Cummer et al.*, 2009]. The ISUAL instrument aboard FORMOSAT II observed GJs mostly over tropical oceans [*Chen et al.*, 2008a]. The present case, however, was produced by a mid-latitude, low-topped winter thunderstorm.

[32] On 12 December 2009, Europe was under the influence of a large high pressure area (at sea level) centered over Scotland. A shallow low pressure distribution was present over the Mediterranean area. Cold air near the surface was transported into southern Europe by northeasterly winds. At the 500 hPa level (5.4 km altitude) a west-east oriented trough descended from eastern France into the northern Mediterranean Sea, lowering the temperatures at that level to values around −30°C, while 2 meter and 850 hPa (1.4 km altitude) temperatures stayed relatively warm, 9–12°C and 0°C, respectively. The steep drop of temperature with height led to conditional instability, a situation in which a volume ("parcel") of air from near the ground becomes warmer (lighter) than surrounding air after lifting to saturation, and will accelerate up to the altitude where the environment becomes warmer again (the equilibrium level). The Global Forecast System weather model calculated less than 300 J kg^{-1} Convective Available Potential Energy (CAPE, described in meteorology textbooks, e.g., *Wallace and Hobbs* [1973], p. 345). This is a measure of buoyant energy, which affects updraft speed and turbulent mixing. From observational experience, this value is on the low side compared to most western Mediterranean fall thunderstorm situations (but similar to CAPE values in the eastern Mediterranean as reported by *Ganot et al.* [2007]). Much higher values (up to several thousands J kg^{-1}) regularly occur in other parts of the world. Low level winds converged into a small low pressure area west of the GJ location, and rising motions predicted by the model were present over a deep layer. Several cells with lightning developed between Corsica and the coast of France.

[33] The radiosonde and hodograph of 00 UTC on 13 December 2009 of Ajaccio, Corsica, Figure 9, reveals that the flow was rather weak and its direction turning clockwise with height through the lowest 3 km, topped by an intense jetstream of 30–40 m s^{-1} just above the equilibrium level of the convection. Temperature lapse rates were dry-adiabatic (near 10° per km) over the lowest 3000 m, facilitating rapid upward acceleration of parcels into charge-generating temperature regions at <−10°C and colder. The soundings displays the parcel trajectory (dashed curve) based on the most-unstable parcel, excluding the nocturnal surface inversion which was unlikely to exist over sea. This is also supported by GFS model output. 0–6 km wind vector difference, a measure referred to as deep layer shear in severe storm forecasting, was 31 m s^{-1}, and storm-relative helicity over 0–3 km was 135 m^2 s^{-2}. Such hodographs and values are commonly associated with supercells [e.g., *Rasmussen and Blanchard*, 1998], intense storms with rotating updrafts, of which low-topped versions are known to exist [*Markowski and Straka*, 2000, and references therein]. The large distance between the storm and the radar precludes a more detailed analysis. Evidence against the supercell hypothesis comes from not having any concentrated detections of lightning as would be typical for an intense graupel core, although it cannot be ruled out that there were undetected intracloud discharges.

[34] Although this situation could be characterized as "cold season maritime thunderstorms," this was not a typical situation. Normally, rounds of sprites and elves are produced over numerous small convective cells or clusters when Atlantic depressions, followed by a cold airmass, enter the Mediterranean Sea from the west or northwest in fall and winter. In such cases, the CAPE tends to occur away from thermal gradients and the jetstream, in areas devoid of vertical wind shear. In infrared channels of Meteosat images, typical convective activity consists of clearly cellular white (cold) shapes, while in the present case, the cells were embedded in a gray (warmer) contiguous area of stratiform cloud associated with the front between the warm Mediterranean and the continental cold airmass.

[35] Figure 2 shows that the detected flash at 2336:56.556, during the first GJ frame (26), occurred near the coldest cloud top of −34°C, with a cloud top altitude (6.5 km, near 425 hPa in Figure 9) apparently above the calculated equi-

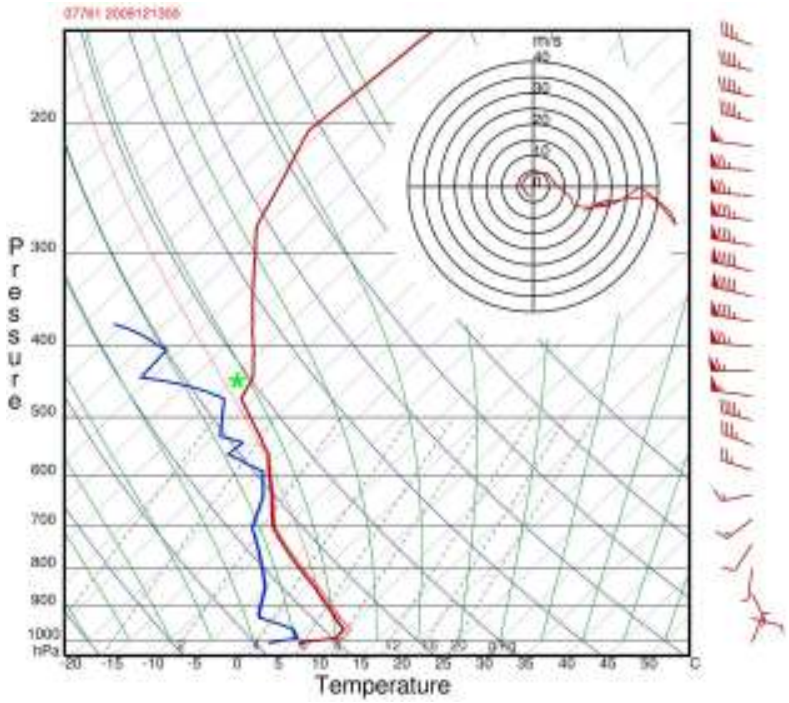

Figure 9. Meteorological sounding of Ajaccio (Corsica) at 00 UTC on 13 December 2009, showing a profile of temperature (right red curve), dewpoint (left blue curve) and wind vanes (two full dashes mean ~10 m s^{-1}, triangle means ~25 m s^{-1}) against pressure on the vertical axis in a Skew-T thermodynamic diagram. The calculated most-unstable parcel ascent trajectory is drawn in red. The approximate cloud top level of the storm (−34°C) is marked by a green star. The 500 hPa level was at an altitude of 5430 m, 400 hPa at 7010 m. Temperature lines run from lower left to upper right. The circular diagram is a hodograph showing the u and v components of the wind in m s^{-1} for every pressure level, starting at the ground on the left.

librium level, which was approximately at the −30°C level in the GFS model. So, the overshooting storm top was penetrating into the jet stream, with winds around 70 knots (36 m s^{-1}) indicated in the Ajaccio sounding. Radar images from Sardinia (Figure 10) at 210 km distance also showed a well-defined convective core, but cannot resolve more detailed features due to the radar beam width and scanning altitude. The images show the storm was not special in terms of reflectivity values and size, but it is of interest that the highly reflective core of the storm corresponds well to the GJ location and was more intense at 2300 UTC than at 2330 UTC.

[36] Figure 11 shows the evolution of cloud top temperature area within the region marked in Figure 2. The storm was virtually stationary for several hours before and after the GJ. In particular, cloud tops colder than −30°C were expanding continuously since 2100 UTC and reached a maximum area at 2330 UTC, just before the GJ. The coldest cloud tops at the position of the GJ were slightly warming, which is in agreement with the decreasing intensity of radar reflectivity. Lightning flash rates in the region (Figure 12) were on average 58 flashes per hour, 58% of them positive polarity. Among these a relatively high number of +CG flashes had peak currents greater than 100 kA (39 in 7 hours). Such numbers would be remarkable compared to summer situations but are not uncommon for maritime winter thunderstorms [e.g., *Soula et al.*, 2010; *Hayakawa et al.*, 2004]. The highest amplitude +CG flash, reported by LINET as 406 kA, but missed by the EUCLID network, occurred at 2341:07 UTC, four minutes after the GJ and at a location very close to the likely GJ position. It produced an exceptionally bright elve and a sprite. Figure 12 shows that the rate of detected flashes in the storm was very low between 23:09 and 23:36 UTC. During this period only four flash "sequences" [*Soula et al.*, 2009, 2010] occurred, southwest of the GJ. Between 2305:27 and 2336:56 no activity was detected in the smaller subregion around the GJ (42.0°N, 7.6°E ± 0.1°). Activity was resumed after the GJ. During the silent period, the cloud may have accumulated more charge than usual.

7. Discussion

[37] The gigantic jet (GJ) discussed in this article contributes to a growing population of observations of this rare phenomenon, first documented in 2002. While *Su et al.* [2003] documented five GJs occurring within a period of only 20 minutes, and *van der Velde et al.* [2007b] documented two GJs from two separate cloud tops within a few minutes, most GJs appear as rather isolated events, unlike sprites and elves, and thus the details of their morphology and any associated electromagnetic signals, and the variation therein, are yet being slowly uncovered.

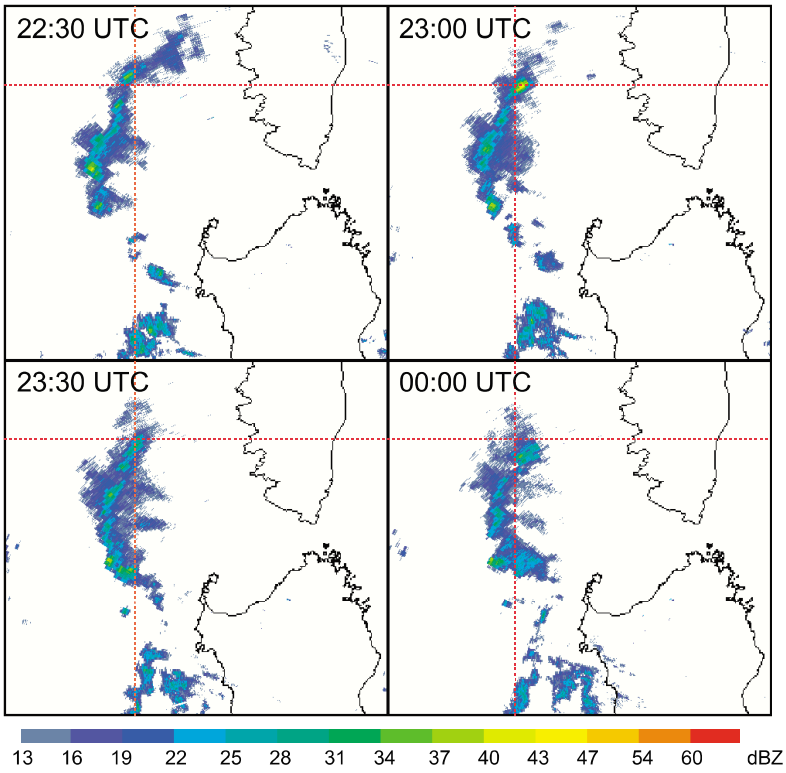

Figure 10. Long-range base scan reflectivity images from the radar operated by ARPAS Dipartimento Specialistico Regionale Idrometeoclimatico, at Monte Rosu, Sardinia, about 210 km to the southeast of the gigantic jet. The radar scanned the storm at approximately 4.1 km altitude. The red lines offer reference for the motion of the storm, their crossing point is the approximate location of the gigantic jet.

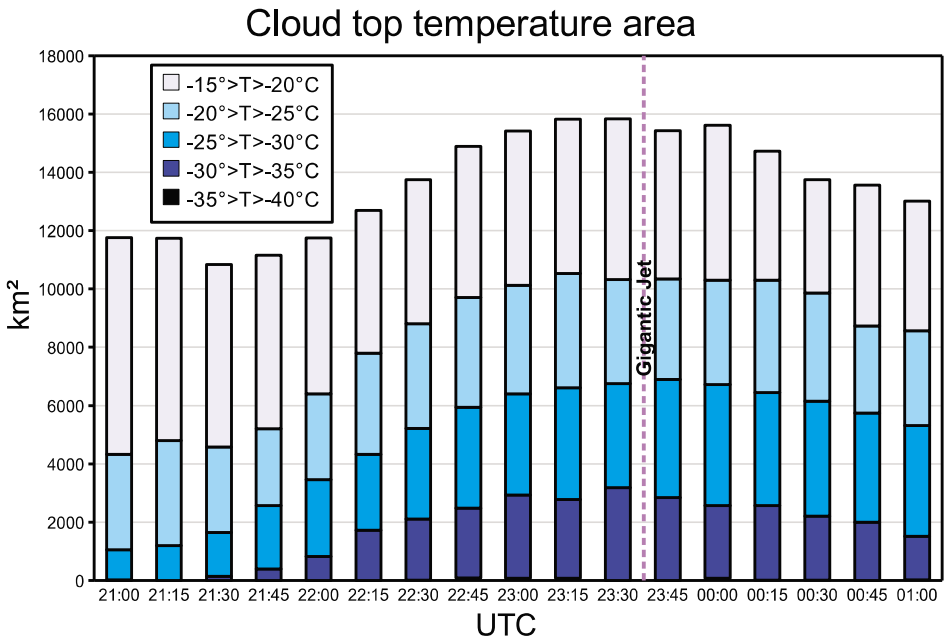

Figure 11. Evolution of Meteosat cloud top temperature area of different temperature intervals, within the box shown in Figure 2.

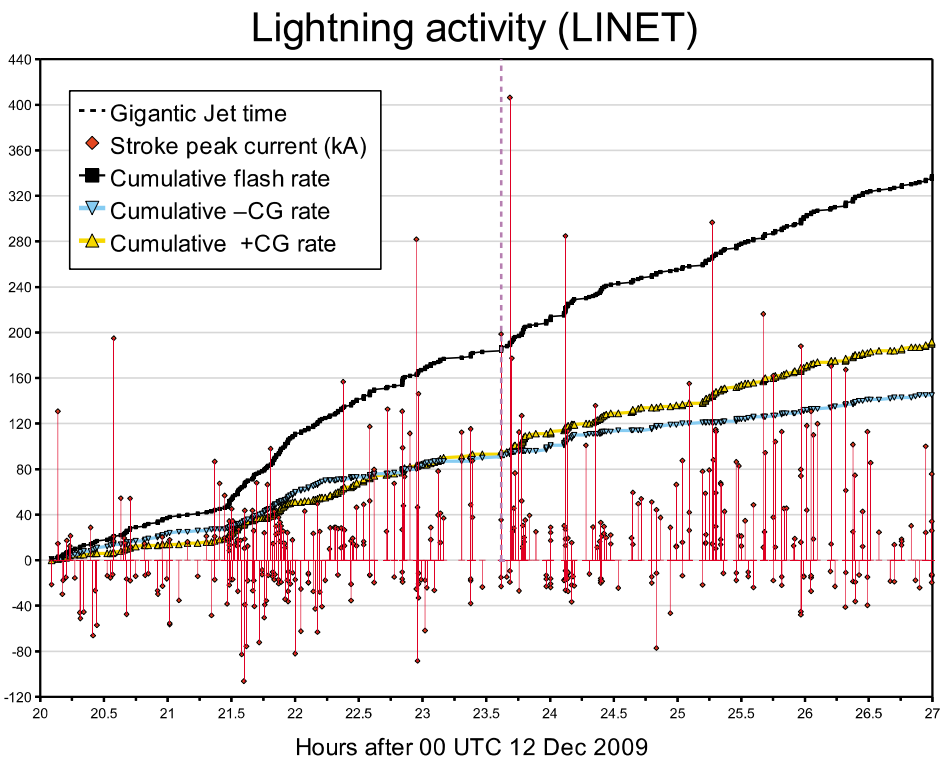

Figure 12. Cumulative lightning flash rates over time (curves) and peak currents in kA (red spikes), as detected by LINET within the box shown in Figure 2.

[38] The present case demonstrates that GJs can also be produced by low-topped maritime winter thunderclouds. It was the first GJ confirmed to transfer a large quantity of negative charge from the ionosphere to the cloud by upward positive streamers, and it was accompanied by a sprite with a halo. The GJ reached a top altitude of about 91 km within less than 40 ms, and featured a trailing jet and bright transition region lasting 80–120 ms at altitudes between 49 and 59 km. These top and transition altitudes match very well with previous observations. However, the diameter of this event was larger than others. The leading jet started narrow (~3.7 km) and tripled in width during the trailing jet stage (11 km), almost to the same size of the bright transition zone. In contrast, the Marfa, Texas, GJ [*van der Velde et al.*, 2007a] and the two Broken Arrow, Oklahoma, GJs [*van der Velde et al.*, 2007b] were narrower and did not broaden during the trailing jet phase. They neither appeared as bright as the present GJ.

[39] The large diameter and brighter appearance of this GJ could be related to the presence of a large current measured by various ultra to very low frequency receiver stations: a maximum of ~3.3 kA (current moment of 280 kA km), integrated to ~136 C of charge (total charge moment change of 11600 C km). The waveforms indicated for the first time a positive cloud-to-ionosphere discharge (+CI), i.e., the event acted to transfer electrons from high altitudes into the positive cloud charge. Previous GJ events were of −CI polarity [*Cummer et al.*, 2009; *Su et al.*, 2003; *Pasko et al.*, 2002 with further details by *Krehbiel et al.*, 2008; *Hsu et al.*, 2004] or missed a clear association with any ultra/extremely low frequency signal [*van der Velde et al.*, 2007a, 2007b; *Su et al.*, 2003 (one event)]. While the charge moment change was very comparable to that of the −CI event by *Cummer et al.* [2009], the charge transfer (144 C over 75 km) in their event lasted longer at a lower current, up to 730 A, compared to 3300 A (136 C over 85 km) in the event studied here. So, the efficiency of charge transfer was at least 4.5 times greater in the present event. The +CI polarity implies a difference in characteristics of the upward streamers (positive polarity) and the charge-gathering leaders (negative polarity) inside the cloud, compared to −CI events. *Williams* [2006] reviewed the asymmetry in positive and negative streamer (and leader) behavior and their consequences for bidirectional discharges. Positive streamers can be initiated and sustained in a weaker ambient electric field than negative streamers. Their propagation is smoother than that of negative streamers (leaders). Differences in upward streamer speed, degree of branching, current magnitude and duration (i.e. charge transfer efficiency) can be expected, similar to CG flashes of different polarities. In CGs, efficient transfer of charge by strong, long-lasting continuing currents is more common in +CG flashes than in −CG discharges, which tend to have multiple brief strokes separated by tens of milliseconds, which can prolong the discharge process [*Mazur*, 2002; *Williams*, 2006]. The short duration of this efficient +GJ event (~120 ms) contrasts with the long duration of several previously reported −GJs (>300 ms, *Kuo et al.* [2009]; 800 ms, *Pasko et al.* [2002]; and >400 ms, *Su et al.* [2003]), so it appears that the events with (stronger) negative-upward currents last longer, but clearly more evidence is needed (in particular: more observations of +GJs).

[40] Very interesting is the second part of the ultra low frequency waveforms and its relation to the visual processes occurring in the trailing jet and sprite. The positive current attributed to the gigantic jet (P1 in Figure 5) reached a minimum, then started increasing again 23 ms before the +CG (period P2 in Figure 5) to similar current moments as before. It is possible that this was indeed an increase of current inside the GJ as the discharge tapped a new positive cloud charge source, similar to an M-component [*Campos et al.*, 2009]. This current could have continued also during the +CG current in the other direction, since opposite magnetic fields can cancel each other. It is likely that the rebrightening of the top of the trailing jet in frame 29 (the sprite frame) was an effect of the measured continuing current surge within the jet. Additionally the quasi-electrostatic field or the electromagnetic pulse of the +CG could have caused rebrightening. In some cases, rebrightening has been reported in sprites after new +CGs [*Stenbaek-Nielsen et al.*, 2000], but more often new streamers grow without rebrightening the adjacent older parts (personal observation of the first author). Also the higher beads, which were probably not connected anymore to the trailing jet, were lit up again.

[41] A columniform sprite with halo was triggered by a +CG during the trailing jet stage. The top altitude of this sprite of ~72 km was 5–10 km lower than most other sprites that night, and the diameter of about 60 km, if assumed to be circular, encompasses the location of the GJ. Since the GJ removed considerable charge from the cloud during a long period before the +CG, this could have lowered the sprite initiation height [*Pasko et al.*, 1996; *Li et al.*, 2008] and may have caused the sprite to occur closer to the GJ instead of being centered over the triggering +CG. The direction of the quasi-electrostatic field resulting from the removal of positive charge from the cloud by the GJ is the same as from the following +CG. However, instead of removed to the ground, this positive charge was injected into (or, in other words, electrons were removed from) the stratosphere and mesosphere, leaving positive ions in the wake of upward positive streamers. In frame 29 displayed in Figure 1 it appears as if the sprite elements are slightly tilted (diverging downward) with respect to the vertical grid lines, in accordance with the expected electric field lines around the charge anomaly created by the jet. The details of the relation between the sprite and the GJ is a subject of a forthcoming paper.

[42] The sprite-producing +CG may have been part of the same discharge as the GJ (connected by leaders), or was instead triggered remotely as a neural network by changes in the electric field [*Yair et al.*, 2009]. In turn, two additional CG flashes occurred further to the south within a few hundred ms of the GJ and sprite. Similar rapid sequences of CG flashes spanning tens to hundreds of kilometers within a large stratiform precipitation area in a transient luminous event-producing maritime winter thunderstorm have been reported by *Soula et al.* [2010]. Interestingly, the model by *Riousset et al.* [2010] found that a −CG can be induced by the significant reduction of also the upper charge by the −GJ, leading to enhanced fields between the lower charge layers, however on timescales of tens of seconds rather than the observed hundreds of milliseconds.

[43] Considering that all previously reported GJs occurred over (sub)tropical or mid-latitude thunderstorms with tops in the range of 14–18 km, it is a remarkable observation that a GJ can also be produced, under certain conditions, by the much lower topped maritime winter thunderstorms in mid-latitudes (42°N), which were already well known to produce sprites and elves [e.g., *Takahashi et al.*, 2003; *Ganot et al.*, 2007; *Soula et al.*, 2010]. The storm reached a top of about 6.5 km (at −34°C), less than half that reported for previous GJs. The GJ occurred when the storm was weakening in terms of coldest cloud top and radar reflectivity at 4 km altitude, but when the cold (<−30°C) cloud top area was largest. This could indicate that the charge volume was at a maximum at the time of the event. It is not known, however, how much of the surrounding lower clouds provided charge for the gigantic jet.

[44] The storm top, unlike the rest of the storm, was embedded in the jet stream, which is not typically the case for winter thunderstorms in the Mediterranean. Turbulence induced by the jet stream and its interaction with the storm top may have provoked depletion of the upper charge layer by mixing it with the screening layer at the cloud edge, which creates a situation in which discharges involving the dominant central charge center can escape through the upper charge. This unbalanced charge center mechanism for GJ production was proposed by *Krehbiel et al.* [2008], but no suggestions were given as to which factors control mixing. Alternatively to mixing, the upper negative charge layer could have been transported away (progressively with height) from its opposite polarity lower counterpart by the large difference in wind speed between center and top of the storm. Noninductive charging mechanisms should produce equal amounts of positive and negative charge in the main charge centers well within the cloud (i.e., not affected by entrainment of external or screening charge). So it takes either large amounts of mixed-in screening charge to cancel a significant amount of upper charge, or it requires relative horizontal displacement between charge centers of opposite charge. In relation to the effect of wind shear on electrified clouds, *Levin et al.* [1996] found that the fraction of +CG flashes in winter thunderstorms in Israel increased with the magnitude of wind shear between the 0° and −25°C level. A long, clockwise turning hodograph (meaning large vertical wind shear), as observed in the environment of the storm, is also favorable for generation of significant rotation and strong updrafts in storms, which then can be classified as a supercell. It was not possible to identify this with certainty based on storm structure on radar and satellite images, however, but the cell was long-lived and moved very slowly in a direction to the right of the mean wind over the cloud depth, which matches some characteristics of supercells [e.g., *Browning*, 1964].

[45] Lightning activity in the storm was dominated by positive cloud-to-ground flashes which produced also several sprites and elves. For more than 31 minutes before the GJ, no activity was detected anymore within a range of approximately 10 km around the GJ. Activity was resumed after the GJ. This behavior supports the findings of *Krehbiel et al.* [2008] and *Riousset et al.* [2010] that GJs compete with cloud-to-ground flashes because they tap from the same source. The absence of CG flashes helped accumulate

the required positive charge. *Riousset et al.* [2010] noted that for CGs to cease, the growth of charge in the lowest charge layer must be inhibited somehow. Together with a depleted upper charge region this would favor GJ occurrence. There were two other studies of the CG lightning flash rates near the time of GJ events. *van der Velde et al.* [2007a] reported a relative absence of −CGs around the time of the GJ, and a rapid increase in +CG rates, which could have been intense intracloud flashes, however (peak currents only around 15 kA). If the detected +CG flashes in their Mexican storm were intracloud flashes in a normal polarity storm instead, it would support the conclusions of *Krehbiel et al.* [2008] for initiation of a −GJ. However, in the multicell storm which produced two GJs over Arkansas studied by *van der Velde et al.* [2007b], similar flash rate behavior was reported (not published). Silences in −CG flash rates and significant increases of +CG flash rates were observed minutes before each GJ, but the +CG peak currents were much larger in this storm, so it was impossible to dismiss these as intracloud flashes. So, there is doubt whether those events fit the modeling results for GJs presented by *Krehbiel et al.* [2008] and *Riousset et al.* [2010]. Note that with the lack of triangulated GJ locations, the option is still open that GJs could develop away from storm cores, and emerge e.g. from the electrically more quiescent anvils.

[46] While the presently documented event is the first winter storm GJ reported in scientific literature, it is of interest that Japanese observers, including two high schools [http://sonotaco.jp/forum/viewtopic.php?t=1880] have recorded a large cone-shaped blue jet with a co-located carrot sprite and transition luminosity on 29 November 2008. It came from a low-topped cold front thunderstorm, and the meteorological sounding in that case also revealed strong winds, but through a deep layer, with a similar strong 0–6 km shear (35 m s^{-1}). While we speculate that strong vertical wind shear could have been an important factor in the production of these winter jets, it is still unclear which factors favor the occurrence of gigantic jets in general, including the tropical events produced by much taller storms in a warmer, moister and more unstable environment.

8. Conclusions

[47] This gigantic jet (GJ) was the first ever recorded in Europe. It was produced by a stationary Mediterranean winter thunderstorm west of Corsica with a top of 6.5 km, which was embedded in the jet stream. The strong vertical wind shear is thought to have contributed to the charge imbalance needed for gigantic jet production, e.g. through displacement of the upper negative charge region from the central positive charge region. This was the first gigantic jet determined to be of positive polarity, confirmed by the electromagnetic waveforms of various radio receiver stations. The in-cloud lightning component associated to the GJ was detected as negative polarity flash by one lightning detection system. All evidence supports the mechanism described by *Krehbiel et al.* [2008] of a +GJ originating between the main positive and weakened upper negative charge regions in an inverted-polarity storm.

[48] The event transferred ~136 C of charge within relatively short time (~120 ms), with a peak current of ~3300 A, and was as such the strongest gigantic jet reported to date. An "ultra-slow tail" in the magnetic field waveforms with a duration of 3.5 seconds followed after the event. The event exhibited similar morphology to other events, but was relatively wide and bright. The bright transition region topping the trailing jet, and upper beads were reilluminated, likely in response to a measured second current surge, during which also a positive cloud-to-ground flash (+CG) occurred, 24 km away, triggering a columniform sprite and halo. The sprite elements appeared at a lower altitude than usual, with shorter lengths and wide spacing, and their downward-diverging vertical orientations suggest influence from the altered space charge structure after the gigantic jet. During the completed and trailing stages of the gigantic jet, a patch of light resembling a sprite halo was detected at large altitude or distance from the GJ, further suggesting a large influence of the gigantic jet event on its surrounding environment. Ionospheric D-region conductivity changes produced by the gigantic jet were confirmed for the first time, by monitoring of remote very low frequency (VLF) transmitter signal amplitudes.

Appendix A: Receiver Characteristics

[49]

Duke University [79.09°W, 35.97°N], USA

Recorded field components: BEW, BNS

Magnetic coils are directed to geographic East and to North

Effective passband (A > ~0.7): 0.1–500 Hz (ULF system), 100–25000 Hz (VLF system)

Sampling frequency: 2500 Hz (ULF system), 100000 Hz (VLF system)

Azimuth of the GJ: 55.1696°, Great circle distance of the GJ: 7193 km

Pinon Flat Observatory [116.456°W, 33.61°N], USA

Recorded field components: BEW, BNS

Magnetic coils have been directed to geomagnetic East and to North so deduced directions are corrected with the declination of the station at the time of the installation of the recording system.

Effective passband (A > ~0.7): 0.1–1600 Hz

Sampling frequency: 4096 Hz

Azimuth of the GJ: 38.0162°, Great circle distance of the GJ: 9857 km

CEA station (Commissariat à l'Energie Atomique) [2.63°E, 47.27°N], France

Recorded field components: EZ

Effective passband (A > ~0.7): 1–500 kHz

Sampling frequency: 5 MHz

Azimuth of the GJ: 144.2994°, Great circle distance of the GJ: 706 km

Belsk station [20.8°E, 51.83°N], Poland

Recorded field components: BEW, BNS, EZ

Magnetic coils are directed to East and to North with 1° accuracy

Effective passband (A > ~0.7): 1–34 Hz in HEW, HNS, and 9–33 Hz in EZ

Sampling frequency: 100 Hz

Azimuth of the GJ: 227.4864°, Great circle distance of the GJ: 1479 km

Hornsund station [15.55°E, 77.0°N], Spitzbergen
Recorded field components: BEW, BNS
Magnetic coils are directed to East and to North with 1° accuracy
Effective passband (A > ~0.7): 2.5–24.5 Hz in HEW, HNS
Sampling frequency: 100 Hz
Azimuth of the GJ: 190.2677°, Great circle distance of the GJ: 3911 km

Hylaty station [22.5438°E, 49.2035°N], Poland
Recorded field components: BEW, BNS
The North-South magnetic coil is directed to the geomagnetic North. The declination at the time the coil was installed was +4.3°. The other coil is perpendicular to this.
Effective passband (A > ~0.7): 0.1–52 Hz in HEW, HNS
Sampling frequency: 175.959 Hz
Azimuth of the GJ: 240.9109°, Great circle distance of the GJ: 1408 km

Nagycenk station [16.7167°E, 47.6328°N], Hungary
Recorded field components: BEW, BNS, EZ
Magnetic coils are directed to East and to North with 1° accuracy
Effective passband (A > ~0.7): 2–32 Hz in HEW, HNS, and 4.5–29.5 Hz in EZ
Sampling frequency: 514.27709030213 Hz
Azimuth of the GJ: 232.1530°, Great circle distance of the GJ: 953 km

[50] **Acknowledgments.** The Spanish Ministry of Science and Innovation supported Oscar van der Velde under grant ESP2007-66542-C04-02 and AYA2009-14027-C05-05. The contribution of József Bór was supported by the Hungarian Scientific Research Found (OTKA, support ID K72474). Enrico Arnone acknowledges funding through the European Community's Human Potential Programme Marie Curie under contract MERG-CT-2007–209157. Martin Füllekrug acknowledges support from the Science and Technology Facilities Council under grant PP/E0011483/1 toward the magnetic field recordings at Pinon Flat Observatory, which is operated the Institute of Geophysics and Planetary Physics of the University of California, San Diego. Christos Haldoupis thanks ELKE for providing research support through grant ID 2746. Many scientists have generously contributed data for this study, for which we are grateful to Mariusz Neska (Hornsund and Belsk receiver), Anna Odzimek, Andrezj Kulak and Janusz Mlynarczyk (Hylaty receiver), Nino Amvrosiadi (AWESOME, University of Crete) and Hassen Ghalila (AWESOME, Tunis receiver), Gabriella Sátori (Nagycenk receiver data), Serge Soula and J.P. Olry (satellite data from EUMETSAT/Météo France), Toby Whitley, Torsten Neubert, and Joan Montanyà, Hans-Dieter Betz, Gerhard Diendorfer and A. Mugnai (LINET and EUCLID lightning data), and IMC-ARPAS (Sardinia radar images). We thank Roberto Labanti, Diego Valeri and Renzo Cabassi of the Italian Meteor and TLE Network. Oscar van der Velde acknowledges Pieter Groenemeijer for his radiosonde plotting program.

References

Adachi, T., H. Fukunishi, Y. Takahashi, M. Sato, A. Ohkubo, and K. Yamamoto (2005), Characteristics of thunderstorm systems producing winter sprites in Japan, *J. Geophys. Res.*, *110*, D11203, doi:10.1029/2004JD005012.

Arnone, E., A. Kero, C.-F. Enell, M. Carlotti, C. J. Rodger, E. Papandrea, N. F. Arnold, B. M. Dinelli, M. Ridolfi, and E. Turunen (2009), Seeking sprite-induced signatures in remotely sensed middle atmosphere NO_2: Latitude and time variations, *Plasma Sources Sci. Technol.*, *18*, 034014, doi:10.1088/0963-0252/18/3/034014.

Betz, H.-D., K. Schmidt, P. Oettinger, and M. Wirz (2004), Lightning detection with 3-D discrimination of intracloud and cloud-to-ground discharges, *Geophys. Res. Lett.*, *31*, L11108, doi:10.1029/2004GL019821.

Browning, K. A. (1964), Airflow and precipitation trajectories within severe local storms which travel to the right of the winds, *J. Atmos. Sci.*, *21*, 634–639.

Campos, L. Z. S, M. M. F. Saba, O. Pinto Jr., and M. G. Ballarotti (2009), Waveshapes of continuing currents and properties of M-components in natural positive cloud-to-ground lightning, *Atmospheric Research*, *91*, doi:10.1016/j.atmosres.2008.02.020.

Chapman, F. W., D. Llanwyn Jones, J. D. W. Todd, and R. A. Challinor (1966), Observation on the propagation constant of the Earth-ionosphere Waveguide in the frequency band 8 kc/s to 16 kc/s, *Radio Sci.*, *1*(11), 1273.

Chen, A. B., et al. (2008a), Global distributions and occurrence rates of transient luminous events, *J. Geophys. Res.*, *113*, A08306, doi:10.1029/2008JA013101.

Chen, A. B., et al. (2008b), Meteorological aspects of elves and jets, *Eos Trans. AGU*, *89*(53), Fall Meet. Suppl., Abstract AE13A-0303.

Chou, J., et al. (2007), Blue and gigantic jets from Taiwan 2007 TLE Campaign, *Eos Trans. AGU*, *88*(52), Fall Meet. Suppl., Abstract AE42A-02.

Coleman, L. M., T. C. Marshall, M. Stolzenburg, T. Hamlin, P. R. Krehbiel, W. Rison, and R. J. Thomas (2003), Effects of charge and electrostatic potential on lightning propagation, *J. Geophys. Res.*, *108*(D9), 4298, doi:10.1029/2002JD002718.

Cummer, S. A., J. Li, F. Han, G. Lu, N. Jaugey, W. A. Lyons, and T. E. Nelson (2009), Quantification of the troposphere-to-ionosphere charge transfer in a gigantic jet, *Nature Geoscience*, doi:10.1038/ngeo607.

Cummins, K. L., M. J. Murphy, E. A. Bardo, W. L. Hiscox, R. B. Pyle, and A. E. Pifer (1998), A combined TOA/MDF technology upgrade of the U. S. National Lightning Detection Network, *J. Geophys. Res.*, *103*(D8), 9035–9044.

Dowden, R. L., J. B. Brundell, and C. J. Rodger (2002), VLF lightning location by time of group arrival (TOGA) at multiple sites, *J. Atmos. Sol.-Terr. Phys.*, *64*, 817–830.

Eastin, M. D., and M. C. Link (2009), Miniature supercells in an offshore outer rainband of Hurricane Ivan (2004), *Mon. Weather Rev.*, *137*, 2081–2104.

Füllekrug, M., A. C. Fraser-Smith, and S. C. Reising (1998), Ultra-slow tails of sprite-associated lightning flashes, *Geophys. Res. Lett.*, *25*(18), 3497–3500.

Füllekrug, M., C. Price, Y. Yair, and E. R. Williams (2002), Intense oceanic lightning, *Ann. Geophys.*, *20*, 133–137.

Ganot, M., Y. Yair, C. Price, B. Ziv, Y. Sherez, E. Greenberg, A. Devir, and R. Yaniv (2007), First detection of transient luminous events associated with winter thunderstorms in the eastern Mediterranean, *Geophys. Res. Lett.*, *34*, L12801, doi:10.1029/2007GL029258.

Haldoupis, C., N. Amvrosiadi, B. R. T. Cotts, O. A. van der Velde, O. Chanrion, and T. Neubert (2010), More evidence for a one-to-one correlation between *Sprites* and *Early* VLF perturbations, *J. Geophys. Res.*, *115*, A07304, doi:10.1029/2009JA015165.

Hayakawa, M., T. Nakamura, Y. Hobara, and E. Williams (2004), Observation of sprites over the Sea of Japan and conditions for lightning-induced sprites in winter, *J. Geophys. Res.*, *109*, A01312, doi:10.1029/2003JA009905.

Hsu, R., et al. (2004), Transient luminous jets recorded in the Taiwan 2004 TLE campaign, *Eos Trans. AGU*, *85*(47), Fall Meet. Suppl., Abstract AE31A-0151.

Hu, W., S. A. Cummer, and W. A. Lyons (2007), Testing sprite initiation theory using lightning measurements and modeled electromagnetic fields, *J. Geophys. Res.*, *112*, D13115, doi:10.1029/2006JD007939.

Inan, U. S., S. A. Cummer, and R. A. Marshall (2010), A survey of ELF and VLF research on lightning-ionosphere interactions and causative discharges, *J. Geophys. Res.*, *115*, A00E36, doi:10.1029/2009JA014775.

Kanamori, T., Y. Takahashi, T. Adachi, A. Ohkubo, K. Yamamoto, M. Sato, and S. A. Cummer (2004), Blue jet and grafted sprites observed in summertime, Japan, *Eos Trans. AGU*, *85*(47), Fall Meet. Suppl., Abstract AE31B-0162.

Krehbiel, P. R., J. A. Riousset, V. P. Pasko, R. J. Thomas, W. Rison, M. A. Stanley, and H. E. Edens (2008), Upward electrical discharges from thunderstorms, *Nature Geoscience*, doi:10.1038/ngeo162.

Kuo, C.-L., et al. (2009), Discharge processes, electric field, and electron energy in ISUAL-recorded gigantic jets, *J. Geophys. Res.*, *114*, A04314, doi:10.1029/2008JA013791.

Levin, Z., Y. Yair, and B. Ziv (1996), Positive cloud-to-ground flashes and wind shear in Tel-Aviv thunderstorms, *Geophys. Res. Lett.*, *23*(17), 2231–2234.

Li, J., S. A. Cummer, W. A. Lyons, and T. E. Nelson (2008), Coordinated analysis of delayed sprites with high-speed images and remote electromagnetic fields, *J. Geophys. Res.*, *113*, D20206, doi:10.1029/2008JD010008.

Lyons, W. A., M. A. Stanley, T. E. Nelson, S. A. Cummer, G. R. Huffines, and K. C. Wiens (2008), Supercells and Sprites, *Bull. Amer. Meteor. Soc.*, *89*, 1165–1174.

Mansell, E. R., D. R. MacGorman, C. L. Ziegler, and J. M. Straka (2002), Simulated three-dimensional branched lightning in a numerical thunderstorm model, *J. Geophys. Res.*, *107*(D9), 4075, doi:10.1029/2000JD000244.

Markowski, P. M., and J. M. Straka (2000), Some observations of rotating updrafts in a low-buoyancy, highly sheared environment, *Mon. Weather Rev.*, *128*(2), 449–461.

Mazur, V. (2002), Physical processes during development of lightning flashes, *Comptes Rendus Phys.*, *3*, 1393–1409.

Mazur, V., and L. Ruhnke (1998), Model of electric charges in thunderstorms and associated lightning, *J. Geophys. Res.*, *103*(D18), 23,299–23,308.

Neubert, T. (2003), On sprites and their exotic kin, *Science*, *300*, 747.

Neubert, T., et al. (2008), Recent results from studies of electric discharges in the mesosphere, *Surv. Geophys*, *29*(2), 71–137, doi:10.1007/s10712-008-9043-1.

Orville, R. E. (1999), Comments on "Large peak current cloud-to-ground lightning flashes during the summer months in the contiguous United States," *Mon. Weather Rev.*, *127*, 1937–1938.

Pasko, V. P. (2008), Blue jets and gigantic jets: Transient luminous events between thunderstorm tops and the lower ionosphere, *Plasma Phys. Controlled Fusion*, *50*, 124050, doi:10.1088/0741-3335/50/12/124050.

Pasko, V. P., U. S. Inan, and T. F. Bell (1996), Sprites as luminous columns of ionization produced by quasi-electrostatic thundercloud fields, *Geophys. Res. Lett.*, *23*(6), 649–652.

Pasko, V. P., M. A. Stanley, J. D. Mathews, U. S. Inan, and T. G. Wood (2002), Electrical discharge from a thundercloud top to the lower ionosphere, *Nature*, *416*, 152–154, doi:10.1038/416152.

Petrov, N. I., and G. N. Petrova (1999), Physical mechanisms for the development of lightning discharges between a thundercloud and the ionosphere, *Tech. Phys. Lett.*, *44*, 472–475.

Raizer, Y. P., G. M. Milikh, and M. N. Shneider (2007), Leader–streamers nature of blue jets, *J. Atmos. Sol. Terr. Phys.*, *69*, 925–938, doi:10.1016/j.jastp.2007.02.007.

Rasmussen, E. N, and D. O. Blanchard (1998), A Baseline Climatology of Sounding-Derived Supercell and Tornado Forecast Parameters, *Weather and Forecasting*, *13*, 4, 1148–1164.

Riousset, J. A., V. P. Pasko, P. R. Krehbiel, W. Rison, and M. A. Stanley (2010), Modeling of thundercloud screening charges: Implications for blue and gigantic jets, *J. Geophys. Res.*, *115*, A00E10, doi:10.1029/2009JA014286.

Rust, W. D., and T. C. Marshall (1996), On abandoning the thunderstorm tripole charge paradigm, *J. Geophys. Res.*, *101*, 23,499–23,504.

Sentman, D. D., H. C. Stenbaek-Nielsen, M. G. McHarg, and J. S. Morrill (2008), Plasma chemistry of sprite streamers, *J. Geophys. Res.*, *113*, D11112, doi:10.1029/2007JD008941.

Shalimov, S., and T. Bösinger (2008), On distant excitation of the ionospheric Alfvén resonator by positive cloud-to-ground lightning discharges, *J. Geophys. Res.*, *113*, A02303, doi:10.1029/2007JA012614.

Soula, S., O. van der Velde, J. Montanya, T. Neubert, O. Chanrion, and M. Ganot (2009), Analysis of thunderstorm and lightning activity associated with sprites observed during the EuroSprite campaigns: Two case studies, *Atmos. Res.*, *91*, 514–528, doi:10.1016/j.atmosres.2008.06.017.

Soula, S., O. van der Velde, J. Palmieri, J. Montanya, O. Chanrion, T. Neubert, F. Gangneron, Y. Meyerfeld, F. Lefeuvre, and G. Lointier (2010), Characteristics and conditions of production of transient luminous events observed over a maritime storm, *J. Geophys. Res.*, *115*, D16118, doi:10.1029/2009JD012066.

Stenbaek-Nielsen, H. C., and M. G. McHarg (2008), High time-resolution sprite imaging: observations and implications, *J. Phys. D: Appl. Phys.*, *41*, 234009, doi:10.1088/0022-3727/41/23/234009.

Stenbaek-Nielsen, H. C., D. R. Moudry, E. M. Wescott, D. D. Sentman, and F. T. S. Sabbas (2000), Sprites and possible mesospheric effects, *Geophys. Res. Lett.*, *27*(23), 3829–3832.

Stenbaek-Nielsen, H. C., R. Haaland, M. G. McHarg, B. A. Hensley, and T. Kanmae (2010), Sprite initiation altitude measured by triangulation, *J. Geophys. Res.*, *115*, A00E12, doi:10.1029/2009JA014543.

Stolzenburg, M., W. D. Rust, and T. C. Marshall (1998), Electrical structure in thunderstorm convective regions, 3. Synthesis, *J. Geophys. Res.*, *103*(D12), 14,097–14,108, doi:10.1029/97JD03545.

Su, H. T., et al. (2003), Gigantic jets between a thundercloud and the ionosphere, *Nature*, *423*, 974–976, doi:10.1038/nature01759.

Takahashi, Y., R. Miyasato, T. Adachi, K. Adachi, M. Sera, A. Uchida, and H. Fukunishi (2003), Activities of sprites and elves in the winter season, Japan, *J. Atmos. Sol.-Terr. Phys.*, *65*(5), 551–560, doi:10.1016/S1364-6826(02)00330-9.

Tsai, L. Y., et al. (2009), Blue jets over tropical cyclones, AGU Chapman Conference on Effects of Thunderstorms and Lightning in the Upper Atmosphere, University Park, Pennsylvania, USA.

van der Velde, O. A., W. A. Lyons, T. E. Nelson, S. A. Cummer, J. Li, and J. Bunnell (2007a), Analysis of the first gigantic jet recorded over continental North America, *J. Geophys. Res.*, *112*, D20104, doi:10.1029/2007JD008575.

van der Velde, O. A., W. A. Lyons, S. A. Cummer, M. B. Cohen, D. D. Sentman, N. Jaugey, T. E. Nelson, and R. Smedley (2007b), Electromagnetical, Visual and Meteorological Analyses of two Gigantic Jets Observed Over Missouri, USA, *Eos Trans. AGU*, *88*(52), Fall Meet. Suppl., Abstract AE23A-0895.

van der Velde, O. A., J. Montanyà, S. Soula, N. Pineda, and J. Bech (2010), Spatial and temporal evolution of horizontally extensive lightning discharges associated with sprite-producing positive cloud-to-ground flashes in northeastern Spain, *J. Geophys. Res.*, *115*, A00E56, doi:10.1029/2009JA014773.

Wallace, J. M., and P. V. Hobbs (1973), Atmospheric Science, An Introductory Survey, International Geophysics, vol. 92, 2nd ed., 504 pp., Academic Press, New York, NY.

Wescott, E. M., Jr. (1996), Blue starters: Brief upward discharges from an intense Arkansas thunderstorm, *Geophys. Res. Lett.*, *23*(16), 2153–2156.

Wescott, E. M., D. Sentman, D. Osborne, D. Hampton, and M. Heavner (1995), Preliminary results from the Sprites94 aircraft campaign: 2. Blue jets, *Geophys. Res. Lett.*, *22*(10), 1209–1212.

Wescott, E. M., D. D. Sentman, M. J. Heavner, D. L. Hampton, and O. H. Vaughan Jr. (1998), Blue Jets: Their relationship to lightning and very large hailfall, and physical mechanisms for their production, *J. Atmos. Sol. Terr. Phys.*, *60*(7–9), 713–714, doi:10.1016/S1364-6826(98)00018-2.

Wescott, E. M., D. D. Sentman, H. C. Stenbaek-Nielsen, P. Huet, M. J. Heavner, and D. R. Moudry (2001), New evidence for the brightness and ionization of blue starters and blue jets, *J. Geophys. Res.*, *106*(A10), 21549–21554.

Williams, E. (1998), The positive charge reservoir for sprite-producing lightning, *J. Atmos. Sol.-Terr. Phys.*, *60*, 689–92.

Williams, E. R. (1989), The tripole structure of thunderstorms, *J. Geophys. Res.*, *94*, 13151–13167.

Williams, E. R. (2006), Problems in lightning physics—The role of polarity asymmetry, *Plasma Sources Sci. Technol.*, *15*, S91–S108.

Yair, Y., C. Price, M. Ganot, E. Greenberg, R. Yaniv, B. Ziv, Y. Sherez, A. Devir, J. Bor, and G. Satori (2008), Optical observations of transient luminous events associated with winter thunderstorms near the coast of Israel, *Atmos. Res.*, *91*, doi:10.1016/j.atmosres.2008.06.018.

Yair, Y., R. Aviv, and G. Ravid (2009), Clustering and synchronization of lightning flashes in adjacent thunderstorm cells from lightning location networks data, *J. Geophys. Res.*, *114*, D09210, doi:10.1029/2008JD010738.

E. Arnone, Dipartimento di Chimica Fisica e Inorganica, University of Bologna, Viale Risorgimento 4, 40136 Bologna, Italy.

J. Bór, Geodetic and Geophysical Research Institute of the Hungarian Academy of Sciences, Csatkai Endre u. 6-8, H-9400, Sopron, Hungary.

S. A. Cummer and J. Li, Department of Electrical and Computer Engineering, Duke University, Box 90291, Durham, NC 27708, USA.

T. Farges, Commissariat à l'Energie Atomique, Centre DAM Île-de-France, F-91297, Arpajon, France.

M. Füllekrug, Centre for Space, Atmospheric and Oceanic Science, Department of Electronic and Electrical Engineering, University of Bath, BA2 7AY, Bath, United Kingdom.

C. Haldoupis, Physics Department, University of Crete, Heraklion, GR-71003 Crete, Greece.

S. NaitAmor, Centre de Recherche en Astronomie Astrophysique & Géophysique, Route de l'Observatoire B.P 63, Bouzareah, Algiers 16340, Algeria.

O. A. van der Velde, Department of Electrical Engineering, Technical University of Catalonia, C/Colom 1, 08222, Terrassa, Barcelona, Spain. (oscar.van.der.velde@upc.edu)

F. Zanotti, Italian Meteor and TLE Network, Ferrara, Italy.